Optimization of 3D Coverage Layout for Multi-UAV Collaborative Lighting in Emergency Rescue Operations

Dan Jiang[1], Rui Yan[2]*
Beijing Municipal Commission of Housing and Urban-Rural Development Beijing, China[1]
School of Economics and Management, University of Science and Technology Beijing, Beijing, China[2]

***Abstract*—In emergency rescue scenarios, Unmanned Aerial Vehicles (UAVs) play a pivotal role in navigating complex terrains and high-risk environments. This paper proposes an optimization model for the three-dimensional coverage layout of a multi-UAV collaborative lighting system, specifically designed to meet the spatial requirements of emergency operations. An enhanced Particle Swarm Optimization (PSO) algorithm is employed to tackle the layout challenges, featuring adaptive inertia weights and asymmetric learning factors to improve both efficiency and global search capabilities. The simulation results demonstrate that the proposed method significantly enhances coverage efficiency, achieving over 90% coverage in critical areas while ensuring precise UAV positioning. Additionally, the algorithm shows faster convergence and stronger global search ability, effectively optimizing UAV deployment and improving operational efficiency during rescue missions. This study offers a practical and reliable layout solution for multi-UAV collaborative lighting systems, which is crucial for reducing rescue times, ensuring operational safety, and improving resource allocation in emergency responses.**

Keywords*—Unmanned Aerial Vehicles; emergency rescue; collaborative lighting; three-dimensional coverage; particle swarm algorithm

I. Introduction

Geological disasters are increasingly prevalent worldwide, with the Global Disaster Data Platform reporting 392 wildfires, 109 earthquakes, and 109 floods in the last six months alone [1]. These statistics likely underestimate the true frequency of such events. The sudden and unpredictable nature of these disasters, coupled with complex environmental conditions, poses significant challenges for emergency rescue operations. Issues such as injuries to personnel, transportation difficulties, and disruptions in communication, power, and lighting infrastructure complicate these efforts further.

In this context, UAVs have emerged as crucial tools in managing such crises. UAVs, which do not require an onboard human presence, offer flexibility, efficiency, and convenience, proving especially useful in confined spaces, complex environments, or hazardous conditions. Their deployment can significantly reduce rescue times, enhance operational efficiency, and improve post-disaster relief efforts [2]. UAVs have broad applications across various sectors such as agriculture, construction, transportation, emergency rescue, military operations, and collaborative lighting [3].

The use of UAVs is particularly critical in emergency rescue situations where traditional lighting equipment may fail to provide rapid and effective illumination [4]. A collaborative approach using multiple UAVs can achieve more flexible and efficient lighting solutions. This paper focuses on optimizing the three-dimensional coverage layout of UAVs equipped with lighting systems, which play pivotal roles in emergency scenarios by enhancing lighting conditions, expanding coverage areas, improving safety, easing workload, and offering flexibility to adapt to diverse mission requirements.

The contributions of this paper include enhancing the comprehensiveness and inclusiveness of the 3D coverage model through innovative UAV technology that depicts disaster scenes and obstacle locations, optimizing 3D lighting coverage using an advanced particle swarm optimization algorithm to improve calculation accuracy and efficiency, and providing a comprehensive discussion on the role of UAV lighting systems in rescue operations. This optimization aids in reducing rescue times, ensuring the safety of rescuers, and minimizing the consumption of resources.

The structure of the paper is organized as follows: Section II reviews related literature; Section III develops the 3D coverage model for the lighting system; Section IV introduces the enhanced particle swarm optimization algorithm; Section V presents a computational study with examples and numerical results; Section VI concludes the paper.

II. Literature Review

A. Current Development of UAVs and their Applications in Different Scenarios

Over the past few decades, UAVs have rapidly evolved, transitioning from their initial military use to various civilian applications. One of the research areas receiving significant attention from scholars is the application of UAVs in emergency rescue scenarios. Different types of emergency rescue UAVs can be utilized for ground site exploration, thermal imaging search and rescue, rescue site mapping, and manned evacuations. In emergency rescue operations, UAVs offer valuable support for information gathering and complex environment rescue due to their compact size, flexibility, and user-friendliness [5]. Moreover, the modular design of UAVs enables the attachment of different systems tailored to specific emergency scenarios, increasing the range of rescue missions.

UAV applications are rapidly expanding across multiple domains. In the realm of smart cities and public safety, UAVs serve as versatile mobile platforms for smart city applications and security surveillance. The utilisation of UAVs and vehicles for last-mile urban deliveries represents an innovative delivery approach. This delivery model's optimisation problem is recognized as the UAV Travelling Salesman Problem (TSP-D). El-Adle et al. [6] studied a deterministic last-mile delivery problem by designing heuristic algorithms based on mixed integer programming to efficiently and accurately prioritise customers for UAV deliveries. Li et al. [7] introduced trucks and a UAV routing model (TDRP-FT) that considers flight altitude selection and time windows. The TDRP-FT model is validated using a hybrid algorithm that combines a greedy stochastic adaptive search process and an adaptive large-neighbourhood search to assess its effectiveness [8].

UAVs can significantly enhance urban public safety by offering early warning and support in diverse emergency scenarios and security operations. Based on BeiDou satellite positioning technology and Lora communication technology, [9] proposed a method of using multiple single-target trackers to replace part of the yolov3 detection task,[10] and put forward the design idea and specific implementation scheme of the vehicle monitoring prediction model.

Urban UAV route planning is a pivotal challenge, involving the quest for an optimal flight path under specific conditions. Miao et al. [11] proposed an improved symbiotic organism search algorithm based on the Simple Shape Method (SMSOS) to solve the path planning problem for UAVs, which has faster convergence speed, higher accuracy, and stronger robustness. Cui et al. [12] proposed a UAV trajectory planning scheme based on the hp-adaptive Radau pseudo-spectral method, considering both the dynamics constraints of the UAV and the terrain obstacle constraints during flight, and demonstrated its efficacy. Zhou et al. [13] proposed a mixed-integer linear programming model to address the reinitialized resource-constrained shortest path problem for correcting UAV flight errors. Three pruning strategies are introduced to enhance the effectiveness and efficiency of the algorithm, mitigating the high computational cost associated with the impulse algorithm. Shima and Schumacher [14] adopt a genetic algorithm that efficiently searches the feasible solution space to optimise the combination of multiple UAVs executing collaborative tasks, effectively solving the coupled problem of UAV task assignment and path planning.

UAVs have consistently played a significant role in the realm of civil security and disaster response. Most UAV-related research has made significant advancements in the domains of earthquakes, volcanic eruptions, and landslides. Following an earthquake, UAVs can serve as valuable investigative tools for collecting data from buildings that are inaccessible or require inspection. Li et al. [15] introduced an unsupervised method for detecting roof damage using UAV-captured images, which leverage combined color and shape features to assess the earthquake's impact based on the images acquired by UAVs. Thiels et al. [16] investigated the application of UAVs in the transportation of emergency supplies to disaster-stricken areas, hospitals, and offshore vessels during critical situations. Nagasawa et al. [17] proposed a multi-UAV coverage path planning method for 3D reconstruction of damaged buildings after a disaster. By generating, filtering, and ordering camera positioning points around a target damaged building, a final path that balances flight distance and time is provided for each UAV. Guo et al. [18] investigate optimal path planning for UAVs navigating in 3D environments with obstacles. They frame the problem as a nonlinear optimal control problem, incorporating continuous state inequality and terminal equivalence constraints. They propose a control parameterisation-based method to solve it. Ma et al. [19] design specific scenarios to simulate real disaster relief tasks and investigate UAV disaster relief task assignment problems. They propose three algorithms based on the horseshoe crab reagent algorithm: Aggregation-LAL, which utilizes an aggregation mechanism; Dynamic Adjustment-LAL, which employs dynamic adjustment mechanism; and Aggregation and Adjustment algorithms. Results demonstrate that AA-LAL achieves an average 5% improvement in task allocation in special scenarios compared to existing algorithms.

B. Coverage Metrics of the Lighting System in 3D Space

When considering three-dimensional lighting system coverage, the initial consideration is the selection of the light source to enable the measurement of light intensity and range. This paper utilizes LED light sources for illumination in a multi-UAV-carrying lighting system. LED light sources is known for their extended lifespan, compact size, and high luminous efficiency. Research on achieving uniform LED light intensity primarily involves two aspects: the secondary design of the LED light source and optimizing the arrangement and spacing of the LEDs.

The two-dimensional coverage problem has been a prominent subject of prior research in sensor networks. While most studies employ 2D models for network coverage, it is increasingly recognized that these models do not align well with real-world scenarios. Consequently, research on the 3D spatial coverage problem is gaining momentum. Huang et al. [20] (2007) were the first to carry out the research on 3D coverage, and they calculated the coverage by discussing the k-coverage problem. Alam and Haas [21] addressed the problem of 3D coverage and connectivity in underwater networks by dividing the 3D network volume into virtual cells in a distributed and scalable manner and selecting dynamic nodes to achieve perceptual coverage. The scheme can be used to achieve k-coverage. Gou et al. [22] proposed an energy efficient coverage enhancement method VKECE - 3D based on 3D - Voronoi partitioning and K - means algorithm, which guarantees the coverage while keeping the number of active nodes to a minimum. VKECE - 3D improves the network coverage and prolongs the network lifetime considerably. Li et al. [23] introduced a novel architecture for wireless sensor networks that incorporated distributed algorithms to manage sensor depths using an adaptive algorithm, resulting in maximal 3D sensor space coverage. Ramesh [24] presented a 3D spatial path planning technique for UAV-based atmospheric environment detection. This method can generate paths with complete coverage and optimal coverage density while accounting for energy constraints. Furthermore, it offers enhanced coverage density when compared to other path generation methods.

Currently, addressing the three-dimensional coverage problem involves mainly either converting the three-dimensional space into a two-dimensional space for computation or developing algorithms specifically designed for three-dimensional space coverage. Nevertheless, achieving accurate coverage calculations in the context of 3D coverage models necessitates more comprehensive and in-depth research efforts.

C. Optimisation Algorithm for the Objective Function

The optimisation of objective functions is a prevalent research area. In recent decades, researchers have developed a range of optimisation algorithms to tackle diverse challenges and problem types.

Classical single-objective optimisation algorithms encompass gradient descent, genetic algorithms, ant colony optimisation, and particle swarm optimisation, among others. Kennedy and Eberhart [25] introduced Particle Swarm Optimisation (PSO), an optimisation algorithm rooted in group intelligence. PSO achieves the search for a globally optimal solution by simulating the collaborative behaviour observed in natural phenomena like bird flocks or fish schools. The application of the particle swarm optimisation algorithm in objective optimisation problems represents an intriguing research avenue.

Nevertheless, the traditional particle swarm algorithm still exhibits shortcomings in terms of global search, diversity, and convergence. Consequently, scholars have conducted research on enhanced particle swarm algorithms. Zhang et al. [26] proposed a new PSO algorithm with self-adaptive inertia weights and social learning strategies, which improves the algorithm's convergence speed and global searching ability by dynamically adjusting the inertia weights and social learning factors ability. Yang et al. [27] proposed a particle swarm optimisation algorithm based on dual search strategies for dynamic multi-objective optimisation. Two search strategies are designed to update the velocity of each particle, which helps to accelerate the convergence speed and maintain the diversity of the population in a dynamic environment. For convergence improvement, Peng et al. [28] proposed a multi-objective particle optimisation algorithm that incorporates the concepts of shared learning and dynamic congestion distance. The algorithm aims to improve the convergence and diversity of the Pareto front by facilitating knowledge sharing among particles and dynamically adjusting the crowding distance metric. Cheng et al. [29] combined an improved non-dominated sorting strategy and a dynamic weight adjustment mechanism to achieve a balance between global search and local convergence, and utilised constraint-handling techniques to deal with constrained problems. For iterative formulation improvement, Lin et al. [30] combined an effective solution set evaluation method based on divergence statistics and a dynamic weight adjustment strategy to achieve a balance between global search and local convergence, and reduced the complexity of the non-dominated ranking by introducing a polynomial fitting function.

III. Model Building

In an emergency rescue scenario, the precise positioning of UAVs represents a critical design consideration. The lighting area must factor in the geographic scenario's influence and the mission requirements to establish a comprehensive rescue area lighting coverage model that incorporates various elements.

A. 3D Coverage Model of the Lighting System

The 3D coverage model produced by the lighting system primarily comprises a 3D cone model. This model represents a cone created in space by the light emitted from the lighting device, with the lighting device serving as the vertex and the base forming a circle, as illustrated in Fig. 1. In this context, the cross-sectional angle of the lighting system is defined as 60°, and the light's range is dependent on the UAV's altitude, simplifying the subsequent coverage rate calculation.

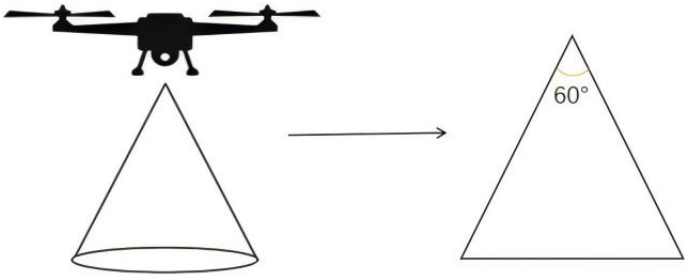

Fig. 1. Three-dimensional conic model of the lighting system and its cross section.

The three-dimensional coverage of the lighting system is initially conceptualized to discretize the volumetric space. However, for practical UAV applications in emergency rescue at specific altitudes, three-dimensional coverage considerations become superfluous. The focus shifts towards two-dimensional plane coverage, which is also subjected to discretization. Within the designated affected area, various characters and obstacles are positioned, necessitating a gridded layout where each grid square denotes a discrete point. Adjustment of the grid step size allows for the manipulation of node positions, facilitating optimal scalability and precision at different accuracy levels. This approach results in the discretization of the two-dimensional plane, as illustrated in Fig. 2, while Fig. 3 visualizes the extent of illumination provided by the two-dimensional lighting system. This model of 3D lighting system coverage effectively simplifies the calculation process, proving highly adaptable for real-world scenarios.

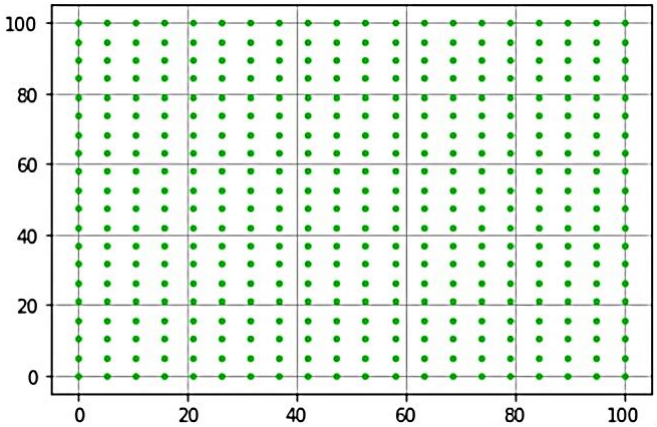

Fig. 2. 2D planar discrete model.

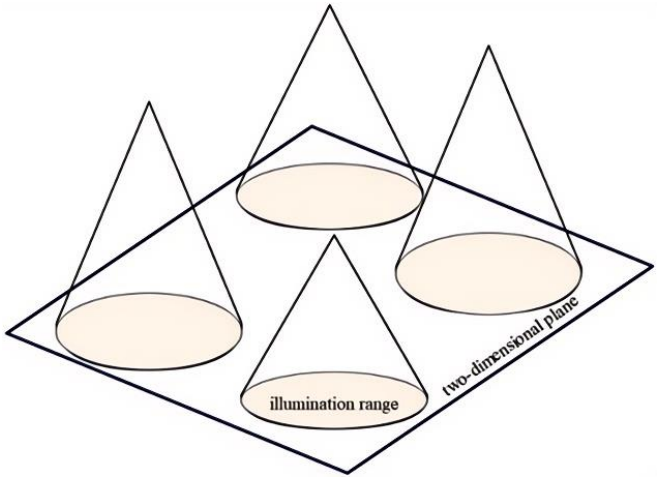

Fig. 3. Multiple unoccupied light ranges in a two-dimensional plane.

B. 3D Geometric Modelling of the Lighting Area

The scheduling of UAVs in rescue scenarios is influenced by lighting requirements and geographic factors. In emergency rescue, the analysis of lighting requirements is centered on providing the necessary illumination to facilitate a range of rescue activities. This analysis necessitates consideration of the specific environmental conditions and site requirements to determine the most suitable lighting solution. It involves detailed examination of the lighting system's type, quantity, placement, intensity, and reliability. Furthermore, emergency rescue lighting demand analysis must address concerns related to energy sources and energy-efficient measures to ensure the stable operation of the lighting system during emergencies.

To meet the specific requirements of emergency rescue operations, the lighting areas are strategically categorized based on the criticality of illumination:

Priority lighting area: This category includes locations crucial for the rescue of individuals or animals, pathways essential for conducting rescue operations, and zones where vital resources are located. It is imperative that the coverage of these areas is meticulously analyzed to ensure at least 90% illumination, serving as a constraint in the optimization challenge.

Other lighting areas: Beyond the priority zones, this category encompasses areas that may contain obstacles, hazardous materials, and miscellaneous regions where maximizing coverage remains a goal.

In outdoor scenarios, the effectiveness of UAV lighting is contingent upon the geographical landscape. For this study, the criteria for adequate coverage in outdoor 3D spatial scenes are defined as follows:

- The affected area must be entirely or partially within the UAV lighting system’s light cone, ensuring clear illumination.
- There must be no obstructions between the UAV system and the target area to avoid shadows and incomplete coverage.

This research concentrates on optimizing the layout of multiple UAVs, deliberately excluding multi-UAV path planning to avoid complexities such as potential collisions. We assume UAVs are deployed to pre-optimized locations, focusing exclusively on layout optimization. This approach allows for a detailed examination and analysis of spatial configuration challenges within multi-UAV systems.

Building on the initial analysis of lighting demands, this study integrates a three-dimensional cone model for the lighting system with a geometric model of the lighting area to establish a comprehensive three-dimensional coverage model, as depicted in Fig. 4. This model not only illustrates the areas covered by light but also applies spatial constraints to calculate precise coverage metrics, enhancing the effectiveness of the UAV lighting strategy in emergency scenarios.

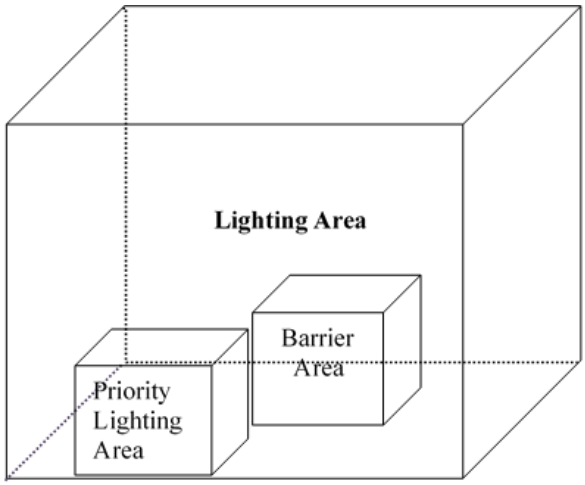

Fig. 4. 3D geometric modelling of lighting areas.

C. Mathematical Modelling

When planning UAV locations, the primary consideration is their ability to adequately illuminate designated areas. In this study, we define a coverage metric as a function with inputs including the 3D coverage model of the lighting system, the 3D geometric model of the illuminated area, the number of UAVs, and the parameters and constraints of the algorithm. The output of this function, the coverage metric, facilitates a comprehensive assessment of the layout's reasonableness, rationality, and effectiveness for the multi-UAV lighting system. The foundational assumptions of the model are:

Uniformity in UAV lighting capabilities: All UAVs are presumed to be equipped with identically capable lighting apparatus, characterized by consistent size, brightness, and irradiation range.

Fixed UAV positions: It is assumed that once each UAV is transported to the designated location and takes off, its position will remain fixed throughout the operation. This implies that our focus is on optimizing the initial layout of UAVs rather than dynamic path planning.

Quantifiable lighting area: The coverage and brightness within the illuminated area are assumed to be quantitatively measurable, allowing for the use of mathematical metrics to evaluate the effectiveness of various lighting configurations, including coverage percentage and brightness uniformity.

Reliability of geographic information: The geographic information employed is presumed accurate and reliable, including details about the area's topography, obstacle locations, and the distribution of critical elements.

No communication interference: It is assumed that there is no communication interference among the UAVs, enabling them to independently execute lighting tasks without the need for real-time communication.

Stable energy supply: A stable energy supply for the UAVs is assumed, ensuring they maintain operational capacity throughout the lighting mission.

1) Definition and meaning of symbols: Identifying constraints and objectives based on the simulated geometric model involves solving a single-objective optimization problem. The variables and parameters used in the model, along with their interpretations, are detailed in Tables I and II.

TABLE I. VARIABLES OF THE THREE-DIMENSIONAL COVERAGE MODEL AND THEIR INTERPRETATION

Variable	Interpretation
$C_i = (x_i, y_i, z_i)$	Geometric position vectors of the UAV
pre_R	Light coverage in priority lighting areas
R_{node}	Node light coverage
R	Total regional light coverage

TABLE II. PARAMETERS OF THE 3D COVERAGE MODEL AND THEIR INTERPRETATION

Parameter	Interpretation
N	Number of UAVs
d	Planar discrete spacing
i	The ith drone
$low_1(x,y,z), up_1(x,y,z)$	Extent of lighting area
$low_2(x,y,z), up_2(x,y,z)$	Range of obstacle locations
$low_3(x,y,z), up_3(x,y,z)$	Scope of Priority Lighting Areas

2) Calculation method of light coverage: Assuming that the lighting region A is a two-dimensional plane, the number of UAVs with the same parameters randomly placed on the region is N, and the coordinates of each UAV are known. The set of UAV nodes is denoted as $C = \{C_1, C_2, \ldots C_N\}$. where $C_i = \{x_i, y_i, z_i\}$ denotes the coordinates of the UAV nodes, and it is also assumed that the light emitted from the illumination system carried by the UAV has a conical top angle of 60°, then the radius of illumination $r = \frac{Z_i}{\sqrt{3}}$.

a) Node set coverage calculation: Assuming that the lighting area A is digitally discretized into $m \times n$ pixels with a discretization spacing of d, the values of m and n are shown in Eq. (1) and (2), respectively.

$$m = (up_1 x - low_1 x) \times d \quad (1)$$

$$n = (up_1 y - low_1 y) \times d \quad (2)$$

Where the coordinate of pixel p is (x, y), then the distance of the pixel from the centre of the drone circle is $d(C_i, p) = \sqrt{(x_i - x)^2 + (y_i - y)^2}$, and defining the event that pixel p is covered by the light from drone i as $r_{i,p}$, the probability of the occurrence of this event, $P_r(r_{i,p})$, is defined as in Eq. (3):

$$P_r(r_{i,p}) = \begin{cases} 1, \iota\phi\ \delta(C_i, p) \le r \\ 0, \text{otherwise} \end{cases} \quad (3)$$

where if $P_r(r_{i,p}) = 1$, it means that pixel point p is covered by the illumination range of UAV i. Therefore, the node coverage is the ratio of the total number of nodes covered by UAVs to the total number of nodes in the region, as in Eq. (4):

$$R_{node} = \frac{\sum_{i=1}^{N} \sum_{p=1}^{m \times n} P_r(r_{i,p})}{m \times n} \quad (4)$$

b) Calculation of area coverage: However, in real-world scenarios, different UAVs may repeatedly cover the same node, requiring the removal of pixel points covered multiple times within the illumination range of multiple UAVs when calculating area coverage. The area coverage of the illuminated region is determined as the ratio of the coverage area of the UAV lighting system to the total area of the illuminated region A, as shown in Eq. (5) and (6):

$$P_{cov(Cov)} = \sum_{p=1}^{m \times n} P_r(r_p) \quad (5)$$

$$\mathrm{R} = \frac{\mathrm{P_{cov(Cov)}}}{\mathrm{m \times n}} \quad (6)$$

where $P_{cov(Cov)}$ denotes the number of unduplicated nodes covered by the UAV lighting system. For any UAV i, if $P_r(r_{i,p}) = 1$, record the node p that is covered by the UAV lighting system at this time and note $P_r(r_p) = 1$. $P_r(r_p) = 1$ indicates that node p is covered by the lighting system.

3) Objective functions and constraints: Coverage problems for UAV node deployment can be divided into two types: area coverage and target coverage. The area coverage focuses on the illumination of the whole area and the target coverage problem focuses on the priority lighting area. The optimisation objective of this problem is to maximise the area coverage as in Eq. (7), P represents the overall coverage rate across the entire region:

$$\mathrm{M}\alpha\xi\ \mathrm{P} \quad (7)$$

Set the constraints of this optimisation problem as:

All UAVs should be located on the surface of the terrain and all inside the area to be illuminated, and secondly, the UAVs must not be inside a three-dimensional obstacle. The UAVs should not be positioned too low, at least three meters above the ground, to avoid interfering with rescue activities, i.e. the coordinates C_i of the UAV satisfy the following Eq. (8):

$$\begin{cases} low_1 x \le x_i \le low_2 x \ or \ up_2 x \le x_i \le up_1 x \\ low_1 y \le y_i \le low_2 y \ or \ up_2 y \le y_i \le up_1 y, i = 1,2,\ldots,N \\ 3 \le z_i \le low_2 z \ or \ up_2 z \le z_i \le up_1 z \end{cases} \quad (8)$$

Avoiding too much repetition of the coverage of different UAV lighting areas, the ratio of the projected distance between any two UAVs on the two-dimensional plane to the sum of their illumination radii is defined to be greater than 0.6, i.e.

satisfying Eq. (9):

$$\sqrt{(x_p - x_q)^2 + (y_p - y_q)^2} > \frac{\sqrt{3}(z_p + z_q)}{5},$$
$$p \neq q, p, q = 1,2,\ldots,N \quad (9)$$

In the disaster area, there are often people or other important things that need to be rescued, so the priority lighting area is established, in which the coverage rate needs to reach more than 90%, defining the coverage rate of the priority lighting area as pre_R, i.e. to satisfy $pre\_R > 0.9$.

IV. Improved Particle Swarm Optimisation Algorithm

This paper employs an enhanced particle swarm algorithm that dynamically adjusts the learning factor and inertia weight factor using diverse methods. It also employs distinct strategies to obtain the individual and global optimal solutions, enhancing search efficiency and accuracy while ensuring a level of stability.

PSO was selected in this study for its simplicity, fast convergence, and strong global search capability. Unlike GA or ACO, PSO does not require complex operations such as crossover or pheromone updating, making it more suitable for time-sensitive emergency rescue scenarios. Additionally, PSO balances exploration and exploitation effectively through adaptive weight adjustments, which aligns well with the requirements of optimizing multi-UAV collaborative lighting layouts.

A. Elementary Particle Swarm Optimisation Algorithm

The core velocity update Eq. (10) and position update Eq. (11) of the elementary particle swarm algorithm can be expressed as follows, respectively:

$$v_{i,d}^{k+1} = wv_{i,d}^{k} + c_1 r_1 \left(x_{i,d,pbest}^{k} - x_{i,d}^{k}\right) + c_2 r_2 \left(x_{d,gbest}^{k} - x_{i,d}^{k}\right) \quad (10)$$

$$x_{i,d}^{k+1} = x_{i,d}^{k} + v_{i,d}^{k+1} \quad (11)$$

where w is the inertia weight, which is used to regulate the global and local search ability of the particle in the search space. c_1 and c_2 are the individual learning factor and the population learning factor, respectively, which are used to regulate the direction and magnitude of the particle updating speed and indicate the magnitude of the learning ability. r_1, r_2 are random numbers of size between 0 and 1, $v_{i,d}^{k}$ is the velocity component of the ith particle in the dth dimension in the kth iteration, $x_{i,d}^{k}$ is the position component of the ith particle in the dth dimension in the kth iteration, $x_{i,d,pbest}^{k}$ is the position component of the individual particle's optimal position of the dth dimension after the kth iteration for the ith particle, and $x_{d,gbest}^{k}$ is the position component of the global optimal position of the dth dimension after the kth iteration. The flow of the optimisation algorithm for particle swarm is shown in Fig. 5.

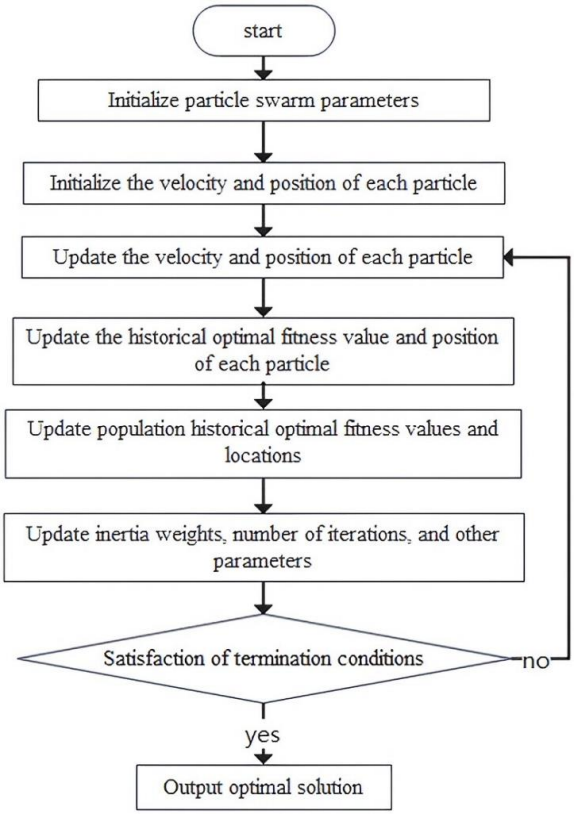

Fig. 5. Particle swarm optimisation algorithm flow.

B. Adjustment of Weights

1) Linearly decreasing inertia weights: In the particle swarm algorithm, the trend of velocity change can be controlled by adjusting the weights w. When w is small, the velocity change of the particle is relatively slow, and it is easy to fall into the local optimal solution; while when w is large, the velocity change of the particle is fast, and it is easy to skip the global optimal solution. Therefore, in order to balance the local search and global search capability, a linearly varying weight strategy is usually adopted, i.e. gradually decreasing from the initial value w_{max} to w_{min}, as shown in Eq. (12), where i is the number of iterations, and i_{max} is the maximum number of iterations.

$$w = w_{max} - (w_{max} - w_{min}) \frac{i}{i_{max}} \quad (12)$$

2) Adaptive inertia weights: The use of adaptive weights in particle swarm optimisation algorithms serves to enhance the algorithm's convergence performance and adaptability. Through dynamic weight adjustments throughout the algorithm's iterations, each particle can more effectively explore the search space and terminate the search more swiftly once the best solution is located.

More specifically, adaptive weights can affect the speed and direction of particle movement towards regions that are more likely to contain the best solution. During the initial stages of the algorithm, larger weights facilitate faster exploration of the search space, whereas in the later stages, smaller weights assist particles in converging more effectively

towards the optimal solution. This dynamic weight adjustment enhances the flexibility and adaptability of the PSO algorithm, enabling it to exhibit improved performance across various problem domains, with the weight changes following the pattern outlined in Eq. (13):

$$w = \begin{cases} w_{min} - (w_{max} - w_{min})\frac{f - f_{min}}{f_{avg} - f_{min}}, f \le f_{avg} \\ w_{max}, f > f_{avg} \end{cases} \quad (13)$$

C. Adjustment of Learning Factors

1) Compression factor method: In particle swarm algorithms, the learning factor is an important parameter used to control the particle speed update. Typically, each particle tracks two historical optimal solutions: the individual historical optimal solution and the neighbourhood historical optimal solution. The learning factors correspond to these two types of historical information, including the individual learning factor c_1 and the social (group) learning factor c_2. Specifically, the individual learning factor controls the extent to which a particle searches near its own historical optimal solution, which makes it more likely that the particle will move in the direction of its own historical optimal solution. The social factor, on the other hand, controls the extent to which a particle searches near its neighbourhood's historical optimal solution, which makes the particle more likely to move towards the neighbourhood's historical optimal solution location. In general, larger individual learning factors facilitated global search, while larger social factors facilitated local search.

In order to effectively control the flight speed of particles and make the algorithm achieve an effective balance between global search and local search, the particle swarm optimisation model that introduces a contraction factor was first proposed by Kennedy and Mendes [19], which employs a compression factor, and this tuning method, by appropriately selecting the parameters, ensures convergence of the particle swarm algorithm and removes the boundary restriction on the speed. The velocity update is formulated as follows in Eq. (14), where the compression factor ϕ is formulated as in Eq. (15).

$$v_{i,d}^{k+1} = \phi[wv_{i,d}^{k} + c_1 r_1\left(x_{i,d,pbest}^{k} - x_{i,d}^{k}\right) + c_2 r_2(x_{d,gbest}^{k} - x_{i,d}^{k})] \quad (14)$$

$$\phi = \frac{2}{\left|2 - (C_1 + C_2) - \sqrt{(C_1 + C_2)^2 - 4(C_1 + C_2)}\right|} \quad (15)$$

2) Asymmetric learning factors: Kennedy proposes an asymmetric learning factor strategy, i.e. the learning factor of each particle is divided into two parts, one part is used for global search and the other part is used for local search. This strategy can make the particles focus more on local search and stop searching faster when the optimal solution is found. The formula of the learning factor is as follows Eq. (16) and Eq. (17), where C_1^{ini} is the initial value of the individual learning factor, C_1^{fin} is the termination value of the individual learning factor, C_2^{ini} is the initial value of the social learning factor, and C_2^{fin} is the termination value of the social learning factor.

$$C_1^k = C_1^{ini} + \left(C_1^{fin} - C_1^{ini}\right)\frac{i}{i_{max}} \quad (16)$$

$$C_2^k = C_2^{ini} + \left(C_2^{fin} - C_2^{ini}\right)\frac{i}{i_{max}} \quad (17)$$

D. Performance Comparison of Different Improvements

In order to verify the effect of the improved algorithm, in the testing process, without setting up the priority lighting area and obstacle area, taking the particle swarm size of 20 and the maximum iteration number of 500, the performance of the algorithm is compared by changing the number of UAVs, the size of the lighting area, and the parameters, interpretation and their specific values of Experiments 1 and 2 are shown in Table III and Table IV, respectively.

TABLE III. THE PARAMETERS, INTERPRETATION AND SPECIFIC VALUES OF EXPERIMENT 1

Parameter	Interpretation	Value
N	Number of UAVs	3
$low_1(x,y,z), up_1(x,y,z)$	Extent of lighting area	(0,0,0),(10,10,10)
$low_1 z, up_1 z$	Altitude range of UAVs	3,7

TABLE IV. THE PARAMETERS, INTERPRETATION AND SPECIFIC VALUES OF EXPERIMENT 2

Parameter	Interpretation	Value
N	Number of UAVs	8
$low_1(x,y,z), up_1(x,y,z)$	Extent of lighting area	(0,0,0),(30,30,30)
$low_1 z, up_1 z$	Altitude range of UAVs	5,10

TABLE V. ALGORITHM PARAMETERS AND THEIR SPECIFIC VALUES

Parameter	Value	Parameter	Value	Parameter	Value	Parameter	Value
w_{max}	0.9	c_1	2	C_1^{ini}	2.5	C_2^{ini}	1
w_{min}	0.4	c_2	2	C_1^{fin}	4.5	C_2^{fin}	2.25

For ease of recording, the modalities of linearly decreasing inertia weights, adaptive inertia weights, compression factor method, and asymmetric learning factor are defined as ordinal numbers 1, 2, 3, and 4, respectively, and for each experiment, one modality is selected among the weights and the learning factor, respectively, to make up four modalities, i.e. 1-3, 1-4, 2-3, and 2-4. The specific values of the parameters of the algorithm in the experiments are shown in Table V, and the iterations of the improved particle swarm algorithm were carried out using the following parameters, using the value of the coverage calculated in the lighting area as the fitness

function, recording the before and after comparisons of the coverage maps obtained from different combinations under different experiments, as well as the corresponding initial fitness value, the optimal fitness value, the average value of fitness, and the variance obtained from the calculation of the fitness.

A comparison of the 2D planar coverage produced by combinations 1-3, 1-4, 2-3, and 2-4 in Experiment 1 is shown below in Fig. 6-9, and a comparison of the algorithmic iterative graphs for the four improvements is shown in Fig. 10.

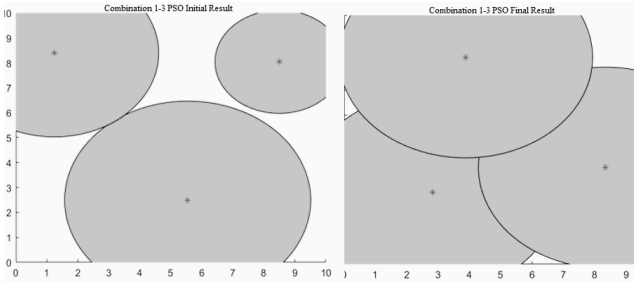

Fig. 6. Experiment 1 Combination 1-3 before and after optimization.

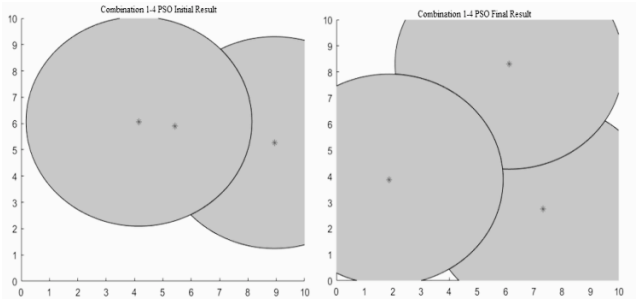

Fig. 7. Experiment 1 Combination 1-4 before and after optimization.

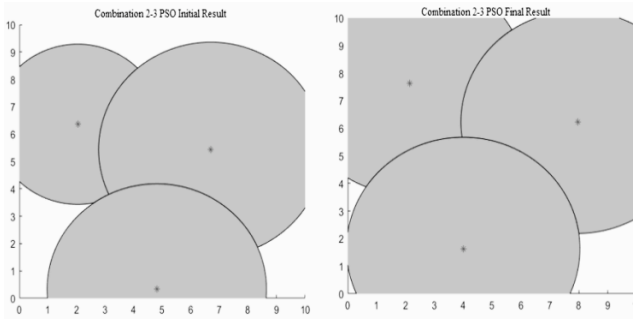

Fig. 8. Experiment 1 Combination 2-3 before and after optimization.

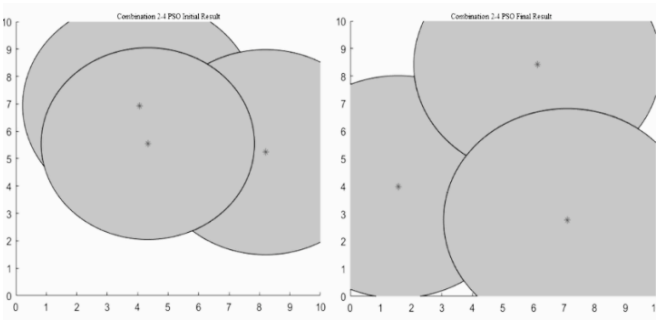

Fig. 9. Experiment 1 Combination 2-4 before and after optimization.

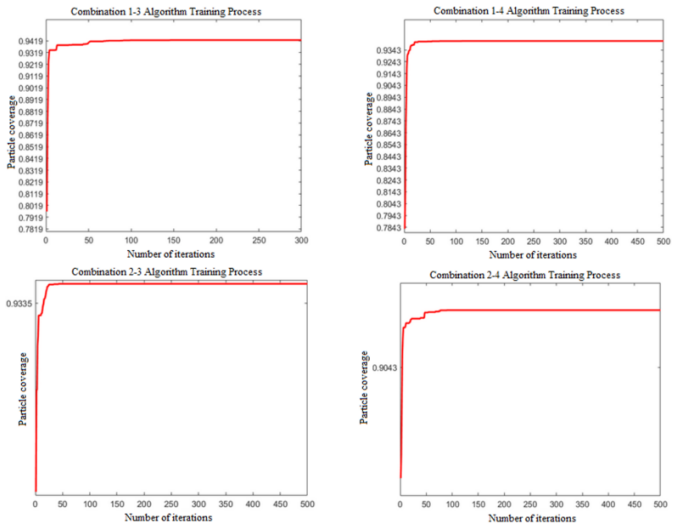

Fig. 10. Experiment 1 Comparison of the iterative process for different combinations.

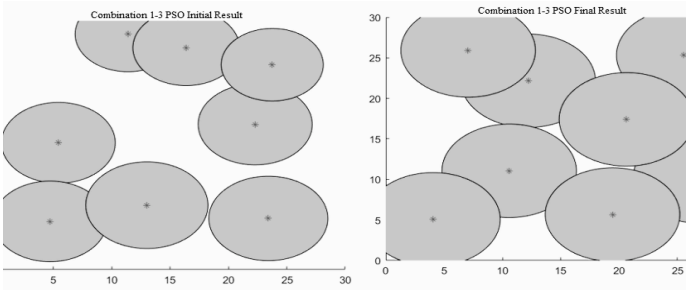

Fig. 11. Experiment 2 Combination 1-3 before and after optimization.

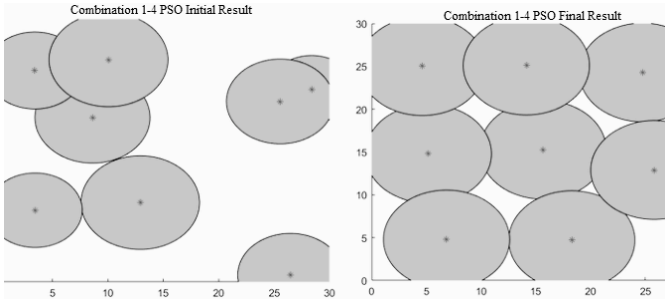

Fig. 12. Experiment 2 Combination 1-4 before and after optimization.

A comparison of the 2D planar coverage produced by combinations 1-3, 1-4, 2-3, and 2-4 in Experiment 2 is shown below in Fig. 11-14, and a comparison of the algorithmic iterative graphs for the four improvements is shown in Fig. 15.

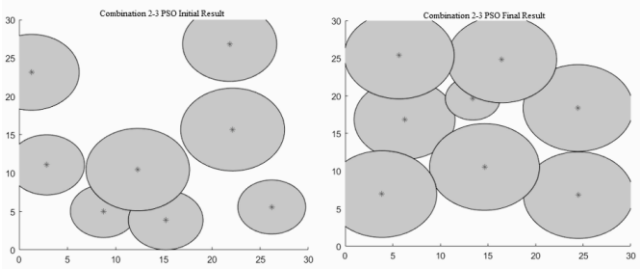

Fig. 13. Experiment 2 Combination 2-3 before and after optimization.

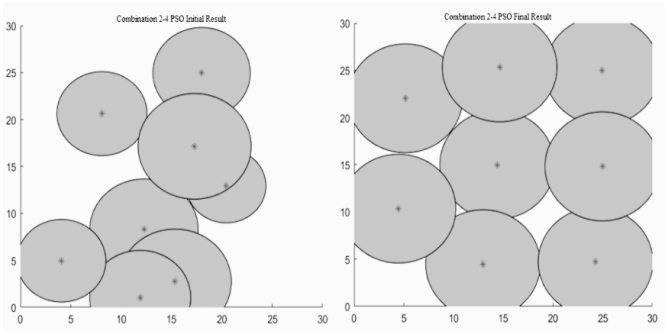

Fig. 14. Experiment 2 Combination 2-4 before and after optimisation.

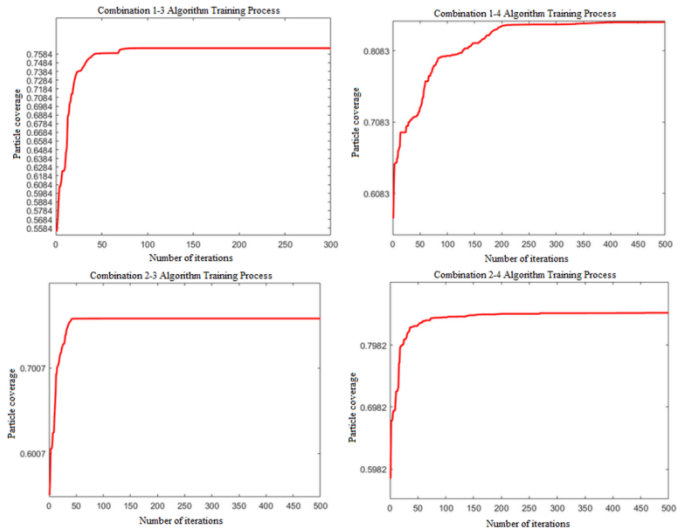

Fig. 15. Experiment 2 Comparison of the iterative process for different combinations.

TABLE VI. PERFORMANCE COMPARISON OF DIFFERENT IMPROVEMENT METHODS

Experiment number	Experimental combinations	Initial fitness	Optimal fitness	Mean fitness	Variance
Experiment 1	1-3	0.751	0.942	0.930	0.0009
	1-4	0.688	0.942	0.912	0.0021
	2-3	0.780	0.939	0.936	0.0008
	2-4	0.687	0.942	0.892	0.0027
Experiment 2	1-3	0.577	0.765	0.747	0.0040
	1-4	0.498	0.849	0.789	0.0067
	2-3	0.497	0.749	0.745	0.0023
	2-4	0.501	0.850	0.801	0.0046

Table VI presents a comparative table of the initial adaptation value, the optimal adaptation value, the average adaptation value, and the variance resulting from adaptation calculations obtained through different experimental improvement methods. From the test results in the table, it is evident that the variance resulting from the experiments is largely consistent and has minimal impact on actual outcomes. However, the approach of utilizing adaptive inertia weights and asymmetric learning factors, specifically the combination of 2-4 in the experiments, yields superior optimisation results compared to other methods. Consequently, a combination of these two enhancement algorithms is employed to address this problem.

V. SIMULATION STUDY

A. Data Preparation

Based on the 3D coverage model of the lighting area, which encompasses the lighting area, priority lighting area, other coverage areas, UAV positions, UAV lighting ranges, and the 2D spatial discrete model, the subsequent 3D model is constructed using the affected area in a real-world scenario, illustrated in Fig. 16.

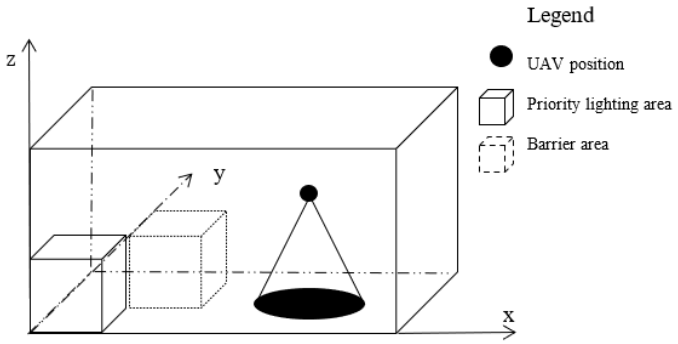

Fig. 16. Lighting area 3D overlay model.

Based on the actual situation of the affected area, the length and width of the lighting area were set at 30 metres and the height at 20 metres, and the specific values of the parameters for the size of the priority lighting area and the obstacle area are shown in Table VII.

TABLE VII. SPECIFIC VALUES FOR THE PARAMETERS OF THE 3D GEOMETRIC MODEL

Parameter	Value	Parameter	Value	Parameter	Value
$low_1(x,y,z)$	(0,0,0)	$low_2(x,y,z)$	(2,2,0)	$low_3(x,y,z)$	(2,0,0)
$up_1(x,y,z)$	(30,30,20)	$up_2(x,y,z)$	(4,4,2)	$up_3(x,y,z)$	(4,2,2)

B. Simulation Results

Assuming that the number of UAVs is 9, the coverage calculation is performed on the lighting areas generated by the nine UAVs, and when the constraints are satisfied, the original UAV positions are entered as the original population to facilitate comparison with the optimised scene. There are nine UAVs in the original scene, and the coverage of the original scene is judged from the calculation of the coverage rate, and the total number of discrete points of 96,100 is obtained by discrete two-dimensional planes with a step size of 0.1, and the lighting of the original scene covers 58,592, with a coverage rate of 0.609, in which the priority lighting area has 900 discrete points, of which 400 are covered, with a coverage rate of 0.444 visible. The initial scene coverage is average and does not meet the desired conditions, of which the illumination coverage area in the 2D plane is shown in Fig. 17.

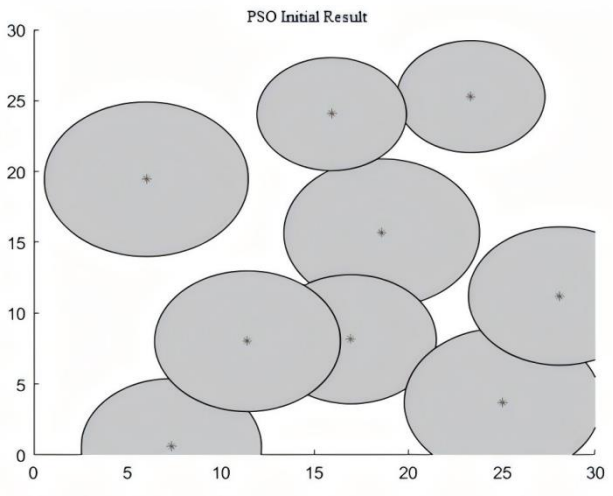

Fig. 17. Particle swarm optimisation algorithm initial coverage results.

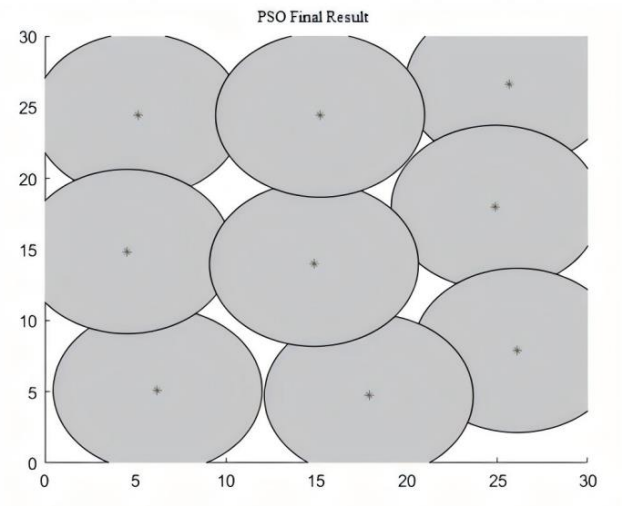

Fig. 18. Optimised 2D coverage map.

Adaptive inertia weights and asymmetric learning factors are chosen to improve the particle swarm algorithm, after the improved particle swarm algorithm is optimised, the coverage nodes are improved compared to the initial scene, by discrete two-dimensional plane with a step size of 0.1, a total of 96,100 discrete points are obtained, and the lighting of the original scene is covered by 86,736, with a coverage rate of 0.903, in which the priority lighting area has a discrete point of 900, of which 900 are covered with a coverage rate of 1. The optimised coverage rate is higher, and at the same time, the UAV positions all satisfy the constraints by not being inside the obstacles, of which the illumination coverage area in the 2D plane is shown in Fig. 18, and the iterative process is shown in Fig. 19. Compared with the simulation experiment without obstacles and priority lighting area, this chapter uses the actual spatial scene for modelling, and the optimisation effect is more realistic. According to the comparison of parameters before and after optimisation, the algorithm is highly effective and adapted to the constraints in emergency rescue, which has a certain degree of universality and can be used in actual rescue with good practical application value.

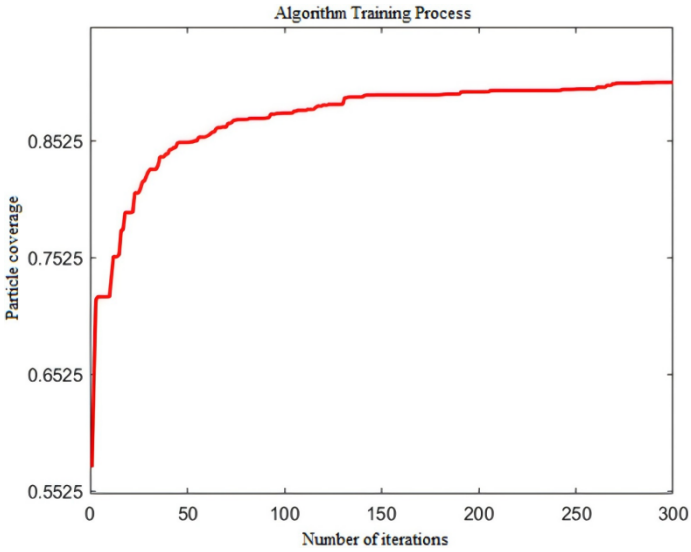

Fig. 19. Algorithmic optimisation process.

C. Effectiveness of the Algorithm

The effectiveness of the improved Particle Swarm Optimization (PSO) algorithm is evident in both the enhanced coverage rate and the optimized UAV deployment strategy.

In the initial UAV layout, the overall coverage rate was 60.9%, with only 44.4% coverage in the priority lighting area. These figures clearly show the inefficiency of the initial deployment, which failed to adequately illuminate critical regions, leaving large portions of the rescue area under-illuminated or overlapping in coverage. After applying the improved PSO algorithm, the overall coverage rate increased significantly to 90.3%, while the priority lighting area achieved a full 100% coverage. This drastic improvement highlights the algorithm's capability to optimize UAV positions effectively, ensuring that crucial rescue areas receive sufficient illumination. This result is crucial for real-world emergency scenarios, where effective lighting directly impacts rescue operations and safety.

The improved PSO algorithm demonstrates superior efficiency in comparison to traditional optimization methods. The adaptive inertia weights allow the algorithm to balance global exploration and local exploitation, preventing premature convergence to suboptimal solutions. Furthermore, the asymmetric learning factors contribute to faster convergence and more accurate UAV positioning, even in complex three-dimensional environments. This is evident from the faster convergence of the algorithm during the simulations, where it reached optimal coverage after fewer iterations compared to traditional methods. For example, in the simulation with 9 UAVs and a step size of 0.1, the optimized algorithm achieved 90.3% coverage with 96,100 discrete points, covering 86,736 points in total. This high coverage, along with improved UAV positioning, ensures that the UAVs avoid obstacles and maximize the effective lighting area.

VI. Conclusion

Collaborative lighting systems involving multiple UAVs can significantly improve the efficiency of accident rescue and

serve as a foundation for informed decision-making during on-site command. The method presented in this study offers an efficient and dependable layout solution for multi-UAV collaborative lighting systems in emergency rescue and related domains. Our research constructs a three-dimensional coverage model of the lighting area based on real-world conditions and addresses the three-dimensional coverage demands of multi-UAV collaborative lighting systems in emergency rescue.

We evaluate the performance of the particle swarm algorithm using various enhancement methods. Adjusting the inertia weights to decrease linearly and modifying the learning factor compression can improve the optimization process, thereby mitigating the particle swarm optimization algorithm's tendency to converge to local optima. This ensures both the speed and accuracy of convergence. Case study results demonstrate that the enhanced particle swarm algorithm effectively optimizes the layout of the multi-UAV lighting system, considering UAV position and coverage area. It guarantees a priority lighting area coverage rate exceeding 90% while ensuring overall lighting coverage.

This study has certain limitations. Firstly, we assumed static UAV positions throughout the operation, without considering dynamic path planning. In real-world emergency scenarios, dynamic factors such as moving obstacles and the need for real-time adjustments to UAV paths may arise, which our current model does not account for. Secondly, the optimization problem addressed in this study is single-objective, focusing solely on maximizing coverage. Important factors such as energy consumption, response time, and the trade-offs between these variables were not incorporated into the model. These assumptions may limit the applicability of the proposed algorithm in more complex rescue scenarios where multiple objectives must be considered simultaneously.

Future research will focus on addressing these limitations. We plan to extend the current model into a multi-objective optimization framework, integrating considerations of energy efficiency, response time, and dynamic path planning. Additionally, the algorithm will be tested in more challenging environments, such as those with dynamic obstacles and changing mission parameters, to validate its robustness and adaptability. Such enhancements will bring the model closer to practical application in real-world emergency rescue missions, where multiple factors influence the success and efficiency of UAV-based lighting systems.

ACKNOWLEDGMENT

This paper was supported by Beijing Natural Science Foundation (Grant No.: 9232022) and Beijing Social Science Foundation Project (Grant No.: 22GLC043).

REFERENCES

[1] Wang, Z. Wu, and Z. Sun, "Optimization of Charging-Station Location and Capacity Determination Based on Optical Storage, Charging Integration, and Multi-Strategy Fusion," J. Green Econ. Low-Carbon Dev., vol. 3, no. 1, pp. 1-14, 2024. https://doi.org/10.56578/jgelcd030101

[2] S. Brischetto and R. Torre, "Preliminary finite element analysis and flight simulations of a modular drone built through fused filament fabrication," J. Compos. Sci., vol. 5, no. 11, p. 293, 2021. https://doi.org/10.3390/jcs5110293

[3] R. Arini, A. D. Putri, W. N. Fadilah, and A. Hasnaoui, "Optimization of Shell and Tube Condenser Effectiveness via PSO Algorithm Coupled with Forced Convection Characterization in Multiphase Systems," Power Eng. Eng Thermophys., vol. 2, no. 4, pp. 188-198, 2023. https://doi.org/10.56578/peet020401

[4] Yahia, A.M., Alkamachi, A. (2024). Design, modeling, and control of tiltable tri-rotors UAV. Journal Européen des Systèmes Automatisés, Vol. 57, No. 3, pp. 841-848. https://doi.org/10.18280/jesa.570323.

[5] H. Hildmann and E. Kovacs, "Using unmanned aerial vehicles (UAVs) as mobile sensing platforms (MSPs) for disaster response, civil security and public safety," Drones, vol. 3, no. 3, p. 59, 2019. https://doi.org/10.3390/drones3030059

[6] A. M. El-Adle, A. Ghoniem, and M. Haouari, "The cost of carrier consistency: Last-mile delivery by vehicle and drone for subscription-based orders," J. Oper. Res. Soc., vol. 75, no. 5, pp. 821-840, 2024. https://doi.org/10.1080/01605682.2023.2210604

[7] H. Li, F. Wang, and Z. Zhan, "Truck and rotary-wing drone routing problem considering flight-level selection," J. Oper. Res. Soc., vol. 75, no. 2, pp. 205-223, 2024. https://doi.org/10.1080/01605682.2023.2185548

[8] Eddine, B.H., Riad, B., Youcef, Z. (2024). Spurious trip rate optimization using particle swarm optimization algorithm. International Journal of Safety and Security Engineering, Vol. 14, No. 1, pp. 63-69. https://doi.org/10.18280/ijsse.140106

[9] J. Liu, J. Wu, and M. Liu, "UAV monitoring and forecasting model in intelligent traffic oriented applications," Comput. Commun., vol. 153, pp. 499-506, 2020. https://doi.org/10.1016/j.comcom.2020.02.009

[10] H. Mhmood, "Design of an Optimized Robust Deadbeat Controller for Roll Motion in Tail-Sitter VTOL UAVs," J. Intell Syst. Control, vol. 3, no. 1, pp. 21-32, 2024. https://doi.org/10.56578/jisc030102

[11] F. Miao, Y. Zhou, and Q. Luo, "A modified symbiotic organisms search algorithm for unmanned combat aerial vehicle route planning problem," J. Oper. Res. Soc., vol. 70, no. 1, pp. 21-52, 2019. https://doi.org/10.1080/01605682.2017.1418151

[12] Y. Cui, X. Fang, G. Liu, and B. Li, "Trajectory optimization of UAV based on Hp-adaptive Radau pseudospectral method," J. Ind. Manag. Optim., vol. 19, no. 1, pp. 675-694, 2022. https://doi.org/10.3934/jimo.2021201

[13] B. Zhou and X. Chen, "A Directional Heuristics Pulse Algorithm for a Two Resources Constrained Shortest Path Problem with Reinitialization," J. Ind. & Manag. Optim., vol. 19, no. 5, pp. 3534-3559, 2023. https://doi.org/10.3934/jimo.2022097

[14] T. Shima and C. Schumacher, "Assigning cooperating UAVs to simultaneous tasks on consecutive targets using genetic algorithms," J. Oper. Res. Soc., vol. 60, no. 7, pp. 973-982, 2009. https://doi.org/10.1057/palgrave.jors.2602617

[15] S. Li, H. Tang, S. He, Y. Shu, T. Mao, J. Li, and Z. Xu, "Unsupervised detection of earthquake-triggered roof-holes from UAV images using joint color and shape features," IEEE Geosci. Remote Sens. Lett., vol. 12, no. 9, pp. 1823-1827, 2015. https://doi.org/10.1109/LGRS.2015.2429894

[16] C. A. Thiels, J. M. Aho, S. P. Zietlow, and D. H. Jenkins, "Use of unmanned aerial vehicles for medical product transport," Air Med. J., vol. 34, no. 2, pp. 104-108, 2015. https://doi.org/10.1016/j.amj.2014.10.011

[17] R. Nagasawa, E. Mas, L. Moya, and S. Koshimura, "Model-based analysis of multi-UAV path planning for surveying postdisaster building damage," Sci. Rep., vol. 11, no. 1, 18588, 2021. https://doi.org/10.1038/s41598-021-97804-4

[18] J. Guo, B. Li, and Y. Ji, "A control parametrization based path planning method for the quad-rotor UAVs," J. Ind. Manag. Optim., vol. 18, no. 2, pp. 1079-1100, 2022. https://doi.org/10.3934/jimo.2021009

[19] X. Ma, D. Wang, N. Zheng, and S. Zhang, "Aggregation and adjustment mechanisms for disaster relief task allocation with uneven distribution," J. Ind. Manag. Optim., vol. 19, no. 3, pp. 1734-1754, 2023. https://doi.org/10.3934/jimo.2022015

[20] C. F. Huang, Y. C. Tseng, and L. C. Lo, "The coverage problem in three-dimensional wireless sensor networks," J. Interconnect. Netw., vol. 8, no. 3, pp. 209-227, 2007.

https://doi.org/10.1142/S0219265907001990

[21] S. N. Alam and Z. J. Haas, "Coverage and connectivity in three-dimensional networks with random node deployment," Ad Hoc Netw., vol. 34, pp. 157-169, 2015. https://doi.org/10.1016/j.adhoc.2014.09.008

[22] P. Gou, B. Guo, M. Guo, and S. Mao, "VKECE-3D: energy-efficient coverage enhancement in three-dimensional heterogeneous wireless sensor networks based on 3D-voronoi and K-means algorithm," Sensors, vol. 23, no. 2, 573, 2023. https://doi.org/10.3390/s23020573

[23] X. Li and X. Y. Zhu, "Design and Testing of Cooperative Motion Controller for UAV-UGV System," Mechatron. Intell Transp. Syst., vol. 1, no. 1, pp. 12-23, 2022. https://doi.org/10.56578/mits010103

[24] Ramesh, N. S. Chandrahas, M. S. Venkatramayya, M. Naresh, P. Talari, D. U. V. D. Prasad, K. S. Kumar, and V. V. Kumar, "Effects of Spacing-to-Burden Ratio and Joint Angle on Rock Fragmentation: An Unmanned Aerial Vehicle and AI Approach in Overburden Benches," Acadlore Trans. Geosci., vol. 2, no. 3, pp. 155-166, 2023. https://doi.org/10.56578/atg020303

[25] J. Kennedy and R. Eberhart, "Particle swarm optimization," Proceedings of ICNN'95 - International Conference on Neural Networks, Perth, WA, Australia, 1995, pp. 1942-1948. https://doi.org/10.1109/ICNN.1995.488968

[26] Y. Zhang, X. Liu, F. Bao, J. Chi, C. Zhang, and P. Liu, "Particle swarm optimization with adaptive learning strategy," Knowl.-Based Syst., vol. 196, 105789, 2020. https://doi.org/10.1016/j.knosys.2020.105789

[27] J. Yang, J. Zou, S. Yang, Y. Hu, J. Zheng, and Y. Liu, "A particle swarm algorithm based on the dual search strategy for dynamic multi-objective optimization," Swarm Evol. Comput., vol. 83, 101385, 2023. https://doi.org/10.1016/j.swevo.2023.101385

[28] G. Peng, Y. W. Fang, W. S. Peng, D. Chai, and Y. Xu, "Multi-objective particle optimization algorithm based on sharing–learning and dynamic crowding distance," Optik, vol. 127, no. 12, pp. 5013-5020, 2016. https://doi.org/10.1016/j.ijleo.2016.02.045

[29] S. Cheng, H. Zhan, and Z. Shu, "An innovative hybrid multi-objective particle swarm optimization with or without constraints handling," Appl. Soft Comput., vol. 47, pp. 370-388, 2016. https://doi.org/10.1016/j.asoc.2016.06.012

[30] Bakirci, M. (2023). A novel swarm unmanned aerial vehicle system: Incorporating autonomous flight, real-time object detection, and coordinated intelligence for enhanced performance. Traitement du Signal, Vol. 40, No. 5, pp. 2063-2078. https://doi.org/10.18280/ts.400524